

Model-independent study for the tau-neutrino electromagnetic dipole moments in $e^+e^- \rightarrow \nu_\tau \bar{\nu}_\tau \gamma$ at the CLIC

A. Gutiérrez-Rodríguez*,¹ M. Köksal†,² A. A. Billur‡,³ and M. A. Hernández-Ruíz§⁴

¹*Facultad de Física, Universidad Autónoma de Zacatecas*

Apartado Postal C-580, 98060 Zacatecas, México.

²*Department of Optical Engineering, Cumhuriyet University, 58140, Sivas, Turkey.*

³*Department of Physics, Cumhuriyet University, 58140, Sivas, Turkey.*

⁴*Unidad Académica de Ciencias Químicas, Universidad Autónoma de Zacatecas*

Apartado Postal C-585, 98060 Zacatecas, México.

(Dated: November 27, 2018)

Abstract

We conduct a study to probe the sensitivity of the process $e^+e^- \rightarrow (\gamma, Z) \rightarrow \nu_\tau \bar{\nu}_\tau \gamma$ to the total cross section, the magnetic moment and the electric dipole moment of the tau-neutrino in a model-independent way. For this study, the beam polarization facility at the Compact Linear Collider (CLIC) along with the typical center-of-mass energies $\sqrt{s} = 380 - 3000 \text{ GeV}$ and integrated luminosities $\mathcal{L} = 10 - 3000 \text{ fb}^{-1}$ is considered. We estimate the sensitivity at the 95% Confidence Level (C.L.) and systematic uncertainties $\delta_{sys} = 0, 5, 10 \%$ on the dipole moments of the tau-neutrino. It is shown that the process under consideration $e^+e^- \rightarrow (\gamma, Z) \rightarrow \nu_\tau \bar{\nu}_\tau \gamma$ is a good prospect for study the dipole moments of the tau-neutrino at the CLIC. Also, our study illustrates the complementarity between CLIC and other e^+e^- and pp colliders in probing extensions of the Standard Model, and shows that the CLIC at high energy and high luminosity provides a powerful means to sensitivity estimates for the electromagnetic dipole moments of the tau-neutrino.

PACS numbers: 14.60.St, 13.40.Em, 12.15.Mm

Keywords: Non-standard-model neutrinos, Electric and Magnetic Moments, Neutral Currents.

* alexgu@fisica.uaz.edu.mx

† mkoksal@cumhuriyet.edu.tr

‡ abillur@cumhuriyet.edu.tr

§ mahernan@uaz.edu.mx

I. INTRODUCTION

Investigations of the theory and phenomenology of neutrino electromagnetic properties continue to be a very active field of interests to both theoretical and experimental physicists. In particular, the study of the Magnetic Moment (MM) and the Electric Dipole Moment (EDM) of the neutrino has been challenging High Energy Physics community, both Theoretical and Experimental in recent decades. In the original formulation of the Standard Model (SM) [1–3] neutrinos are massless particles with zero MM. However, neutrino flavour oscillation experiments from several sources indicate that neutrinos have non-zero mass, which indicates the necessity of extending the SM to accommodate massive neutrinos. In the minimal extension of the SM to incorporate the neutrino mass, the MM of the neutrino is known to be developed in one loop calculation [4, 5], and the non-zero mass of the neutrino is essential to get a non-vanishing MM. Furthermore, the SM predicts CP violation, which is necessary for the existence of the EDM of a variety physical systems. The EDM provides a direct experimental probe of CP violation [6–8], a feature of the SM and beyond the SM (BSM) physics. The signs of new physics can be analyzed by investigating the electromagnetic dipole moments of the tau-neutrino, such as its MM and EDM.

The present best upper limits on the MM and the EDM of the neutrinos, either set directly by experiments or inferred indirectly from observational evidences combined with theoretical arguments, are several orders of magnitude larger than the predictions of the minimal extension of the SM [4, 5, 9]. Therefore, if any direct experimental confirmation of non-zero MM is obtained in the laboratory experiments, it will open a window to new physics. In addition, the dipole moments with the copious amount of neutrinos in the Universe will have significant implications for astrophysics and cosmology, as well as terrestrial neutrino experiments [10, 11]. One of the most sensitive experimental observables to the CP violation BSM is the EDM [12–15]. The search for new sources of CP violation BSM is currently one of the most important fundamental problems of particle physics to be solved. A. Sakharov proposed a solution to this problem [16], the present interaction has to violate a fundamental symmetry of nature: the CP symmetry. The excess of matter over antimatter, or the baryon number asymmetry, was generated in the early Universe by a theory satisfy Sakharov criteria.

Another interesting topics in neutrino physics is to determine its Dirac or Majorana nature. For respond to this, experimentalist are exploring different reactions where the

Majorana nature may manifest [17]. About this topic, the study of neutrino magnetic moments is, in principle, a way to distinguish between Dirac and Majorana neutrinos since the Majorana neutrinos can only have flavor changing, transition magnetic moments while the Dirac neutrinos can only have flavor conserving one.

The anomalous MM of the neutrino are being searched in reactor (MUNU, TEXONO and GEMMA) [18–20], accelerator (LSND) [21, 22], and solar (Super-Kamiokande and Borexino) [23, 24] experiments. The current best sensitivity limits on the MM obtained in laboratory measurements are

$$\mu_{\nu_e}^{exp} = 2.9 \times 10^{-11} \mu_B, \quad 90\% \text{ C.L.} \quad [\text{GEMMA}] \quad [20], \quad (1)$$

$$\mu_{\nu_\mu}^{exp} = 6.8 \times 10^{-10} \mu_B, \quad 90\% \text{ C.L.} \quad [\text{LSND}] \quad [21]. \quad (2)$$

These sensitivity limits exceed by many orders of magnitude the minimally extended SM prediction given by

$$\mu_\nu = \frac{3eG_F m_{\nu_i}}{(8\sqrt{2}\pi^2)} \simeq 3.1 \times 10^{-19} \left(\frac{m_{\nu_i}}{1 \text{ eV}} \right) \mu_B, \quad (3)$$

where $\mu_B = \frac{e}{2m_e}$ is the Bohr magneton [4, 5].

The best world sensitivity bounds for the electric dipole moments d_{ν_e, ν_μ} [25] are:

$$d_{\nu_e, \nu_\mu} < 2 \times 10^{-21} (ecm), \quad 95\% \text{ C.L.} \quad (4)$$

For the τ -neutrino, the bounds on their dipole moments are less restrictive, and therefore it is worth investigating in deeper way their electromagnetic properties. The tau-neutrino correspond to the more massive third generation of neutrinos and possibly possesses the largest mass and the largest MM and EDM. As a consequence, this leaves space for the study of new physics BSM.

A summary of experimental and theoretical limits on the dipole moments of the tau-neutrino are given in Table I of Ref. [26]. See Refs. [9, 27–48] for another limits on the MM and the EDM of the τ -neutrino in different context.

A central goal of the physics programme of the future lepton colliders is to complement the Large Hadron Collider (LHC) results and also search for clues in BSM. The lepton colliders are designed to study the properties of the new particles and the interactions they

might undergo according to the vast amount of theories. Furthermore, the lepton colliders compared to the LHC have a cleaner background, and it is possible to extract the new physics signals from the background more easily. In this regard, there is currently an ongoing effort for the project named the Compact Linear Collider (CLIC) [49–51]. When is constructed and enter into operation, the γe^- and $\gamma\gamma$ collision modes will be studied. The CLIC will be a multi-TeV collider and will be operate in three energy stages, corresponding to center-of-mass energies $\sqrt{s} = 380, 1500, 3000 \text{ GeV}$, and it is an ideal machine to study new physics BSM.

Motivated by the extensive physical program of the CLIC, we conduce a comprehensive study to probe the sensitivity of the process $e^+e^- \rightarrow (\gamma, Z) \rightarrow \nu_\tau \bar{\nu}_\tau \gamma$ to the total cross section, the MM and the EDM of the tau-neutrino in a model-independent way. For the study, the beam polarization facility at the CLIC along with the typical center-of-mass energies $\sqrt{s} = 380, 1500, 3000 \text{ GeV}$ and integrated luminosities $\mathcal{L} = 10, 50, 100, 300, 500, 1000, 1500, 2000, 3000 \text{ fb}^{-1}$ are considered. In addition, we estimate the sensitivity at the 95% *C.L.* and systematic uncertainties $\delta_{sys} = 0, 5, 10 \%$ on the dipole moments of the τ -neutrino. It is shown that the process under consideration $e^+e^- \rightarrow (\gamma, Z) \rightarrow \nu_\tau \bar{\nu}_\tau \gamma$ is a good prospect for study the dipole moments of the tau-neutrino at the CLIC. Furthermore, our study illustrates the complementarity between CLIC and other e^+e^- and pp colliders in probing extensions of the SM, and shows that the CLIC at high energy and high luminosity provides a powerful means to sensitivity estimates for the electromagnetic dipole moments of the tau-neutrino.

The content of this paper is organized as follows: In Section II, we study the total cross section and the dipole moments of the tau-neutrino through the channel $e^+e^- \rightarrow (\gamma, Z) \rightarrow \nu_\tau \bar{\nu}_\tau \gamma$. Finally we conclude in Section III.

II. THE TOTAL CROSS SECTION OF THE PROCESS $e^+e^- \rightarrow \nu_\tau \bar{\nu}_\tau \gamma$ AND DIPOLE MOMENTS

A. Electromagnetic vertex $\nu_\tau \bar{\nu}_\tau \gamma$

Theoretically the electromagnetic properties of neutrinos best studied and well understood are the MM and the EDM. Despite that the neutrino is a neutral particle, neutrinos

can interact with a photon through loop (radiative) diagrams. However, a convenient way of studying its electromagnetic properties on a model-independent way is through the effective neutrino-photon interaction vertex which is described by four independent form factors. The most general expression for the vertex of interaction $\nu_\tau \bar{\nu}_\tau \gamma$ is given in Refs. [52–54]. For the study of the MM and the EDM of the tau-neutrino we following a focusing as the performed in our previous works [26–34, 36–38, 41, 42] with

$$\Gamma^\alpha = eF_1(q^2)\gamma^\alpha + \frac{ie}{2m_{\nu_\tau}}F_2(q^2)\sigma^{\alpha\mu}q_\mu + \frac{e}{2m_{\nu_\tau}}F_3(q^2)\gamma_5\sigma^{\alpha\mu}q_\mu + eF_4(q^2)\gamma_5(\gamma^\alpha - \frac{\not{q}q^\alpha}{q^2}), \quad (5)$$

where e is the electric charge of the electron, m_{ν_τ} is the mass of the tau-neutrino, q^μ is the photon momentum, and $F_{1,2,3,4}(q^2)$ are the four electromagnetic form factors of the neutrino. In general the $F_{1,2,3,4}(q^2)$ are independent form factors, and they are not physical quantities, but in the limit $q^2 \rightarrow 0$ they are quantifiable and related to the static quantities corresponding to charge radius, MM, EDM and anapole moment (AM) of the Dirac neutrinos, respectively [44, 55–60]. In this paper we study the anomalous MM μ_{ν_τ} and the EDM d_{ν_τ} of the tau-neutrino, which are defined in terms of the $F_2(q^2 = 0)$ and $F_3(q^2 = 0)$ independent form factor as follows:

$$\mu_{\nu_\tau} = \left(\frac{m_e}{m_{\nu_\tau}}\right)F_2(0)\mu_B, \quad (6)$$

$$d_{\nu_\tau} = \left(\frac{e}{2m_{\nu_\tau}}\right)F_3(0), \quad (7)$$

as we mentioned above. The form factors corresponding to charge radius and the anapole moment, are not considered in this paper.

B. Total cross section of the process $e^+e^- \rightarrow \nu_\tau \bar{\nu}_\tau \gamma$ beyond the SM with unpolarized electron-positron beam

The corresponding Feynman diagrams for the signal $e^+e^- \rightarrow (\gamma, Z) \rightarrow \nu_\tau \bar{\nu}_\tau \gamma$ are given in Fig. 1. The total cross section of the process $e^+e^- \rightarrow \nu_\tau \bar{\nu}_\tau \gamma$ with unpolarized electron-positron beam is computed using the CALCHEP 3.6.30 [61] package, which can compute the Feynman diagrams, integrate over multiparticle phase space and event simulation.

Furthermore, in order to select the events we implementing the standard isolation cuts, compatibly with the detector resolution expected at CLIC:

$$\begin{aligned} p_T^\nu &> 150 \text{ GeV}, \\ |\eta^\gamma| &< 2.37, \\ p_T^\gamma &> 150 \text{ GeV}, \end{aligned} \tag{8}$$

we apply these cuts to reduce the background and to optimize the signal sensitivity. In Eq. (8), p_T^ν is the transverse momentum of the final state neutrinos, η^γ is the pseudorapidity and p_T^γ is the transverse momentum of the photon. The outgoing particles are required to satisfy these isolation cuts.

Formally, the $e^+e^- \rightarrow (\gamma, Z) \rightarrow \nu_\tau \bar{\nu}_\tau \gamma$ cross section can be split into two parts:

$$\sigma = \sigma_{BSM} + \sigma_0, \tag{9}$$

where σ_{BSM} is the contribution due to BSM physics, which, in our case it comes from the anomalous vertex $\nu_\tau \bar{\nu}_\tau \gamma$, while σ_0 is the SM prediction. The analytical expression for the squared amplitudes are quite lengthy so we do not present it here. Following the form of Eq. (9), we present numerical fit functions for the total cross section with respect to center-of-mass energy, with unpolarized electron-positron beam and in terms of the independent form factors $F_2(F_3)$.

- For $\sqrt{s} = 380 \text{ GeV}$.

$$\begin{aligned} \sigma(F_2) &= [(2.68 \times 10^{11})F_2^4 + (1.97 \times 10^4)F_2^2 + 0.041](pb), \\ \sigma(F_3) &= [(2.68 \times 10^{11})F_3^4 + (1.97 \times 10^4)F_3^2 + 0.041](pb). \end{aligned} \tag{10}$$

- For $\sqrt{s} = 1.5 \text{ TeV}$.

$$\begin{aligned} \sigma(F_2) &= [(3.32 \times 10^{13})F_2^4 + (5.13 \times 10^5)F_2^2 + 0.012](pb), \\ \sigma(F_3) &= [(3.32 \times 10^{13})F_3^4 + (5.13 \times 10^5)F_3^2 + 0.012](pb). \end{aligned} \tag{11}$$

- For $\sqrt{s} = 3 \text{ TeV}$.

$$\begin{aligned}\sigma(F_2) &= [(1.49 \times 10^{14})F_2^4 + (9.70 \times 10^5)F_2^2 + 0.003](pb), \\ \sigma(F_3) &= [(1.49 \times 10^{14})F_3^4 + (9.70 \times 10^5)F_3^2 + 0.003](pb).\end{aligned}\tag{12}$$

It is worth mentioning that in equations for the total cross section (10)-(12), the coefficients of $F_2(F_3)$ given the anomalous contribution, while the independent terms of $F_2(F_3)$ correspond to the cross section at $F_2 = F_3 = 0$ and represents the SM total cross section magnitude.

C. Sensitivity estimates on the μ_{ν_τ} and d_{ν_τ} with unpolarized electron-positron beam

Based on the formulas given by Eqs. (10)-(12), we make model-independent sensitivity estimates for the total cross section of the signal $\sigma_{BSM}(e^+e^- \rightarrow \nu_\tau \bar{\nu}_\tau \gamma) = \sigma_{BSM}(\sqrt{s}, \mu_{\nu_\tau}, d_{\nu_\tau})$, as well as for the anomalous MM μ_{ν_τ} and EDM d_{ν_τ} of the τ -neutrino at the CLIC. To carry out this task, we consider the acceptance cuts given in Eq. (8) and we take into account the systematic uncertainties $\delta_{sys} = 0, 5, 10 \%$ for the collider. In addition, to sensitivity estimates on the parameters of the process $e^+e^- \rightarrow \nu_\tau \bar{\nu}_\tau \gamma$, we use the χ^2 function [26, 27, 48, 62–67]

$$\chi^2 = \left(\frac{\sigma_{SM} - \sigma_{BSM}(\sqrt{s}, \mu_{\nu_\tau}, d_{\nu_\tau})}{\sigma_{SM} \sqrt{(\delta_{st})^2 + (\delta_{sys})^2}} \right)^2, \tag{13}$$

where $\sigma_{BSM}(\sqrt{s}, \mu_{\nu_\tau}, d_{\nu_\tau})$ is the total cross section including contributions from the SM and new physics, $\delta_{st} = \frac{1}{\sqrt{N_{SM}}}$ is the statistical error and δ_{sys} is the systematic error. The number of events is given by $N_{SM} = \mathcal{L}_{int} \times \sigma_{SM}$, where \mathcal{L}_{int} is the integrated CLIC luminosity.

As stated in the Introduction, to carry out our study we considered the typical center-of-mass energies $\sqrt{s} = 380, 1500, 3000 \text{ GeV}$ and integrated luminosities $\mathcal{L} = 10, 50, 100, 300, 500, 1000, 1500, 2000, 3000 \text{ fb}^{-1}$ of the CLIC.

We report in Figs. 2 and 3 the sensitivity on the signal cross section $e^+e^- \rightarrow (\gamma, Z) \rightarrow \nu_\tau \bar{\nu}_\tau \gamma$ at the CLIC as a function of the form factors $F_2(F_3)$ and for different center-of-mass energies $\sqrt{s} = 380, 1500, 3000 \text{ GeV}$. Clearly the total cross section is dominant for $\sqrt{s} = 3000 \text{ GeV}$ and for large values of the form factors $F_2(F_3)$, and decreases as $F_2(F_3)$ tends to zero, recovering the value of the SM as it is shown in Eq. (12).

Sensitivity contours at the 95% *C.L.* in the $F_3 - F_2$ plane for the signal $e^+e^- \rightarrow \nu_\tau \bar{\nu}_\tau \gamma$ with center-of-mass energies $\sqrt{s} = 380, 1500, 3000 \text{ GeV}$ and luminosities $\mathcal{L} = 10, 100, 500, 1500, 3000 \text{ fb}^{-1}$ are given in Figs. 4-6. As highlighted in Fig. 6, the three most sensitive contours for F_2 and F_3 they are the corresponding ones for high energy and high luminosity of $\sqrt{s} = 3000 \text{ GeV}$ and $\mathcal{L} = 3000 \text{ fb}^{-1}$.

As a final result on our sensitivity analysis, we stress the sensitivity estimates on the μ_{ν_τ} and d_{ν_τ} via the channel $e^+e^- \rightarrow \nu_\tau \bar{\nu}_\tau \gamma$ for $\sqrt{s} = 380, 1500, 3000 \text{ GeV}$, $\mathcal{L} = 10, 50, 100, 300, 500, 1000, 1500, 2000, 3000 \text{ fb}^{-1}$, $\delta_{sys} = 0, 5, 10\%$ at 90% *C.L.* and 95% *C.L.*. We show our results in Tables I-III, where the better sensitivity on the dipole moments of the τ -neutrino projected for the CLIC are for $\sqrt{s} = 3000 \text{ GeV}$ and $\mathcal{L} = 3000 \text{ fb}^{-1}$: $|\mu_{\nu_\tau}(\mu_B)| = 2.103 \times 10^{-7}$ and $|d_{\nu_\tau}(ecm)| = 4.076 \times 10^{-18}$ at 90% *C.L.*.

D. Total cross section of the process $e^+e^- \rightarrow \nu_\tau \bar{\nu}_\tau \gamma$ beyond the SM with polarized electron-positron beam

Another option for sensitivity study of the total production of the channel $e^+e^- \rightarrow \nu_\tau \bar{\nu}_\tau \gamma$, in addition the dipole moments of the tau-neutrino, is the electron-positron beam polarization facility at the CLIC. The possibility of using polarized electron and positron beams can constitute a strong advantage in searching for new physics [68]. Furthermore, the electron-positron beam polarization may lead to a reduction of the measurement uncertainties, either by increasing the signal cross section, therefore reducing the statistical uncertainty, or by suppressing important backgrounds. In summary, one another option at the CLIC is to polarize the incoming beams, which could maximize the physics potential, both in the performance of precision tests and in revealing the properties of the new physics BSM.

The general formula for the total cross section for an arbitrary degree of longitudinal e^- and e^+ beams polarization is give by [68]

$$\begin{aligned} \sigma(P_{e-}, P_{e+}) = & \frac{1}{4}[(1 + P_{e-})(1 + P_{e+})\sigma_{++} + (1 - P_{e-})(1 - P_{e+})\sigma_{--} \\ & + (1 + P_{e-})(1 - P_{e+})\sigma_{+-} + (1 - P_{e-})(1 + P_{e+})\sigma_{-+}], \end{aligned} \quad (14)$$

where $P_{e-}(P_{e+})$ is the polarization degree of the electron (positron) beam, while σ_{-+} stands for the cross section for completely left-handed polarized e^- beam $P_{e-} = -1$ and completely

TABLE I: Sensitivity estimates on the μ_{ν_τ} magnetic moment and d_{ν_τ} electric dipole moment via the process $e^+e^- \rightarrow \nu_\tau \bar{\nu}_\tau \gamma$ for $\sqrt{s} = 380 \text{ GeV}$ and $P_{e^-} = P_{e^+} = 0\%$.

90% C.L. $\sqrt{s} = 380 \text{ GeV}$						
$\delta_{sys} = 0\%$			$\delta_{sys} = 5\%$		$\delta_{sys} = 10\%$	
$\mathcal{L} (fb^{-1})$	$ \mu_{\nu_\tau}(\mu_B) $	$ d_{\nu_\tau}(ecm) $	$ \mu_{\nu_\tau}(\mu_B) $	$ d_{\nu_\tau}(ecm) $	$ \mu_{\nu_\tau}(\mu_B) $	$ d_{\nu_\tau}(ecm) $
10	7.953×10^{-6}	1.541×10^{-16}	8.914×10^{-6}	1.727×10^{-16}	1.028×10^{-5}	1.993×10^{-16}
50	6.031×10^{-6}	1.168×10^{-16}	8.225×10^{-6}	1.594×10^{-16}	1.002×10^{-5}	1.943×10^{-16}
100	5.308×10^{-6}	1.028×10^{-16}	8.113×10^{-6}	1.572×10^{-16}	9.988×10^{-6}	1.935×10^{-16}
300	4.285×10^{-6}	8.304×10^{-17}	8.032×10^{-6}	1.556×10^{-16}	9.964×10^{-6}	1.930×10^{-16}
500	3.860×10^{-6}	7.481×10^{-17}	8.016×10^{-6}	1.553×10^{-16}	9.959×10^{-6}	1.929×10^{-16}
95% C.L. $\sqrt{s} = 380 \text{ GeV}$						
$\delta_{sys} = 0\%$			$\delta_{sys} = 5\%$		$\delta_{sys} = 10\%$	
$\mathcal{L} (fb^{-1})$	$ \mu_{\nu_\tau}(\mu_B) $	$ d_{\nu_\tau}(ecm) $	$ \mu_{\nu_\tau}(\mu_B) $	$ d_{\nu_\tau}(ecm) $	$ \mu_{\nu_\tau}(\mu_B) $	$ d_{\nu_\tau}(ecm) $
10	8.417×10^{-6}	1.631×10^{-16}	9.415×10^{-6}	1.824×10^{-16}	1.084×10^{-5}	2.101×10^{-16}
50	6.418×10^{-6}	1.243×10^{-16}	8.700×10^{-6}	1.685×10^{-16}	1.057×10^{-5}	2.048×10^{-16}
100	5.664×10^{-6}	1.097×10^{-16}	8.583×10^{-6}	1.663×10^{-16}	1.053×10^{-5}	2.040×10^{-16}
300	4.593×10^{-6}	8.901×10^{-17}	8.499×10^{-6}	1.647×10^{-16}	1.051×10^{-5}	2.035×10^{-16}
500	4.147×10^{-6}	8.036×10^{-17}	8.482×10^{-6}	1.643×10^{-16}	1.050×10^{-5}	2.034×10^{-16}

right-handed polarized e^+ beam $P_{e^+} = 1$, and other cross sections σ_{--} , σ_{++} and σ_{+-} are defined analogously.

For our sensitivity study, we assuming for definiteness an electron-positron beam polarization $(P_{e^-}, P_{e^+}) = (-80\%, 60\%)$ in the estimated range of the expected CLIC operation setup. Besides the polarized beams we consider the isolation cuts given for Eq. (8).

The numerical fit functions for the total cross sections of the process $e^+e^- \rightarrow \nu_\tau \bar{\nu}_\tau \gamma$, following the form of Eq.(9) with polarized electron-positron beam, and in terms of the independent form factors $F_2(F_3)$ are given by:

TABLE II: Sensitivity estimates on the μ_{ν_τ} magnetic moment and d_{ν_τ} electric dipole moment via the process $e^+e^- \rightarrow \nu_\tau \bar{\nu}_\tau \gamma$ for $\sqrt{s} = 1500 \text{ GeV}$ and $P_{e^-} = P_{e^+} = 0\%$.

90% C.L. $\sqrt{s} = 1500 \text{ GeV}$						
$\delta_{sys} = 0\%$			$\delta_{sys} = 5\%$		$\delta_{sys} = 10\%$	
$\mathcal{L} (fb^{-1})$	$ \mu_{\nu_\tau}(\mu_B) $	$ d_{\nu_\tau}(ecm) $	$ \mu_{\nu_\tau}(\mu_B) $	$ d_{\nu_\tau}(ecm) $	$ \mu_{\nu_\tau}(\mu_B) $	$ d_{\nu_\tau}(ecm) $
10	1.538×10^{-6}	2.980×10^{-17}	1.630×10^{-6}	3.160×10^{-17}	1.826×10^{-6}	3.539×10^{-17}
100	9.145×10^{-7}	1.772×10^{-17}	1.268×10^{-6}	2.458×10^{-17}	1.643×10^{-6}	3.184×10^{-17}
500	6.225×10^{-7}	1.206×10^{-17}	1.209×10^{-6}	2.343×10^{-17}	1.622×10^{-6}	3.143×10^{-17}
1000	5.258×10^{-7}	1.018×10^{-17}	1.201×10^{-6}	2.327×10^{-17}	1.619×10^{-6}	3.138×10^{-17}
1500	4.760×10^{-7}	9.225×10^{-18}	1.198×10^{-6}	2.321×10^{-17}	1.618×10^{-6}	3.136×10^{-17}
95% C.L. $\sqrt{s} = 1500 \text{ GeV}$						
$\delta_{sys} = 0\%$			$\delta_{sys} = 5\%$		$\delta_{sys} = 10\%$	
$\mathcal{L} (fb^{-1})$	$ \mu_{\nu_\tau}(\mu_B) $	$ d_{\nu_\tau}(ecm) $	$ \mu_{\nu_\tau}(\mu_B) $	$ d_{\nu_\tau}(ecm) $	$ \mu_{\nu_\tau}(\mu_B) $	$ d_{\nu_\tau}(ecm) $
10	1.656×10^{-6}	3.210×10^{-17}	1.754×10^{-6}	3.400×10^{-16}	1.960×10^{-6}	3.799×10^{-17}
100	9.921×10^{-7}	1.922×10^{-17}	1.370×10^{-6}	2.656×10^{-17}	1.767×10^{-6}	3.425×10^{-17}
500	6.772×10^{-7}	1.312×10^{-17}	1.307×10^{-6}	2.533×10^{-17}	1.745×10^{-6}	3.382×10^{-17}
1000	5.724×10^{-7}	1.109×10^{-17}	1.298×10^{-6}	2.516×10^{-17}	1.742×10^{-6}	3.377×10^{-17}
1500	5.185×10^{-7}	1.004×10^{-17}	1.295×10^{-6}	2.510×10^{-17}	1.741×10^{-6}	3.375×10^{-17}

- For $\sqrt{s} = 380 \text{ GeV}$.

$$\begin{aligned}
\sigma(F_2) &= [(3.97 \times 10^{11})F_2^4 + (3.16 \times 10^4)F_2^2 + 0.072](pb), \\
\sigma(F_3) &= [(3.97 \times 10^{11})F_3^4 + (3.16 \times 10^4)F_3^2 + 0.072](pb).
\end{aligned} \tag{15}$$

- For $\sqrt{s} = 1.5 \text{ TeV}$.

$$\begin{aligned}
\sigma(F_2) &= [(4.93 \times 10^{13})F_2^4 + (7.23 \times 10^5)F_2^2 + 0.023](pb), \\
\sigma(F_3) &= [(4.93 \times 10^{13})F_3^4 + (7.23 \times 10^5)F_3^2 + 0.023](pb).
\end{aligned} \tag{16}$$

TABLE III: Sensitivity estimates on the μ_{ν_τ} magnetic moment and d_{ν_τ} electric dipole moment via the process $e^+e^- \rightarrow \nu_\tau \bar{\nu}_\tau \gamma$ for $\sqrt{s} = 3000 \text{ GeV}$ and $P_{e^-} = P_{e^+} = 0\%$.

90% C.L. $\sqrt{s} = 3000 \text{ GeV}$						
$\delta_{sys} = 0\%$			$\delta_{sys} = 5\%$		$\delta_{sys} = 10\%$	
$\mathcal{L} (fb^{-1})$	$ \mu_{\nu_\tau}(\mu_B) $	$ d_{\nu_\tau}(ecm) $	$ \mu_{\nu_\tau}(\mu_B) $	$ d_{\nu_\tau}(ecm) $	$ \mu_{\nu_\tau}(\mu_B) $	$ d_{\nu_\tau}(ecm) $
100	4.834×10^{-7}	9.368×10^{-18}	5.593×10^{-7}	1.083×10^{-17}	6.844×10^{-7}	1.326×10^{-17}
500	3.272×10^{-7}	6.341×10^{-18}	4.885×10^{-7}	1.081×10^{-17}	6.532×10^{-7}	1.265×10^{-17}
1000	2.759×10^{-7}	5.348×10^{-18}	4.769×10^{-7}	9.242×10^{-18}	6.489×10^{-7}	1.257×10^{-17}
2000	2.325×10^{-7}	4.506×10^{-18}	4.707×10^{-7}	9.122×10^{-18}	6.468×10^{-7}	1.253×10^{-17}
3000	2.103×10^{-7}	4.076×10^{-18}	4.686×10^{-7}	9.081×10^{-18}	6.460×10^{-7}	1.251×10^{-17}
95% C.L. $\sqrt{s} = 3000 \text{ GeV}$						
$\delta_{sys} = 0\%$			$\delta_{sys} = 5\%$		$\delta_{sys} = 10\%$	
$\mathcal{L} (fb^{-1})$	$ \mu_{\nu_\tau}(\mu_B) $	$ d_{\nu_\tau}(ecm) $	$ \mu_{\nu_\tau}(\mu_B) $	$ d_{\nu_\tau}(ecm) $	$ \mu_{\nu_\tau}(\mu_B) $	$ d_{\nu_\tau}(ecm) $
100	5.254×10^{-7}	1.018×10^{-17}	6.071×10^{-7}	1.176×10^{-17}	7.414×10^{-7}	1.436×10^{-17}
500	3.563×10^{-7}	6.905×10^{-18}	5.309×10^{-7}	1.028×10^{-17}	7.080×10^{-7}	1.371×10^{-17}
1000	3.007×10^{-7}	5.826×10^{-18}	5.183×10^{-7}	1.004×10^{-17}	7.034×10^{-7}	1.363×10^{-17}
2000	2.534×10^{-7}	4.912×10^{-18}	5.116×10^{-7}	9.915×10^{-18}	7.010×10^{-7}	1.358×10^{-17}
3000	2.293×10^{-7}	4.443×10^{-18}	5.093×10^{-7}	9.870×10^{-18}	7.002×10^{-7}	1.357×10^{-17}

- For $\sqrt{s} = 3 \text{ TeV}$.

$$\begin{aligned}
\sigma(F_2) &= [(2.23 \times 10^{14})F_2^4 + (1.43 \times 10^6)F_2^2 + 0.006](pb), \\
\sigma(F_3) &= [(2.23 \times 10^{14})F_3^4 + (1.43 \times 10^6)F_3^2 + 0.006](pb).
\end{aligned} \tag{17}$$

In Eqs. (15)-(17), the coefficients of $F_2(F_3)$ given the anomalous contribution, while the independent terms of $F_2(F_3)$ correspond to the cross section at $F_2 = F_3 = 0$ and represents the SM cross section.

E. Sensitivity estimates on the μ_{ν_τ} and d_{ν_τ} with polarized electron-positron beam

The $e^+e^- \rightarrow \nu_\tau \bar{\nu}_\tau \gamma$ production cross section, as a function of $F_2(F_3)$ projected for the CLIC with polarized electron-positron beam $(P_{e^-}, P_{e^+}) = (-80\%, 60\%)$ and for the center-of-mass energies $\sqrt{s} = 380, 1500, 3000 \text{ GeV}$, they are shown in Figs. 7 and 8. From the direct comparison of Figs. 7 and 8, with their corresponding for the unpolarized case Figs. 2 and 3, a significant gradual increase in the total production cross sections of 0.6, 60 and 100 pb is clearly shown. In addition, the cross section increases with the increase of $F_2(F_3)$, and decreases as $F_2(F_3)$ decreases. The SM result for the production cross section of the reaction $e^+e^- \rightarrow \nu_\tau \bar{\nu}_\tau \gamma$ is obtained in the limit when $F_2(F_3) = 0$. In this case, the terms that depend on $F_2(F_3)$ in Eqs. (15)-(17) are zero and Eqs. (15)-(17) are reduced to the result for the SM.

Taking $(P_{e^-}, P_{e^+}) = (-80\%, 60\%)$, $\sqrt{s} = 380, 1500, 3000 \text{ GeV}$ and $\mathcal{L} = 10, 100, 500, 1500, 3000 \text{ fb}^{-1}$, the contours for estimate the sensitivity of F_2 and F_3 in the $F_2 - F_3$ plane through the reaction $e^+e^- \rightarrow \nu_\tau \bar{\nu}_\tau \gamma$ are evaluated and shown in Figs. 9-11. Fig. 11 illustrates the better sensitivity for F_2 and F_3 with $\sqrt{s} = 3000 \text{ GeV}$, $\mathcal{L} = 10, 500, 3000 \text{ fb}^{-1}$ and $(P_{e^-}, P_{e^+}) = (-80\%, 60\%)$.

Our results are given in Tables IV-VI, in which the sensitivity estimates on the μ_{ν_τ} and d_{ν_τ} via the process $e^+e^- \rightarrow \nu_\tau \bar{\nu}_\tau \gamma$ are shown for $P_{e^-} = -80\%$ and $P_{e^+} = 60\%$, $\sqrt{s} = 380, 1500, 3000 \text{ GeV}$, $\mathcal{L} = 10, 50, 100, 300, 500, 1000, 1500, 2000, 3000 \text{ fb}^{-1}$, $\delta_{sys} = 0, 5, 10 \%$ at 90% C.L. and 95% C.L. The effect of the polarized incoming e^- and e^+ beams shows that the sensitivity on the μ_{ν_τ} and d_{ν_τ} is enhanced by a 5% at $P(-80\%; 60\%)$ polarization configuration, with respect to the unpolarized case (see Tables I-III). Our most relevant results are: $|\mu_{\nu_\tau}(\mu_B)| = 2.002 \times 10^{-7}$ and $|d_{\nu_\tau}(ecm)| = 4.039 \times 10^{-18}$ at 90% C.L.

III. CONCLUSIONS

In this paper, we have sensitivity estimates on the total cross section and on the dipole moments μ_{ν_τ} and d_{ν_τ} through the process $e^+e^- \rightarrow \nu_\tau \bar{\nu}_\tau \gamma$ at the future CLIC. Furthermore, the process is analyzed for two scenarios motivated by the strong advantage in searching for new physics BSM: a) unpolarized electron-positron beam $(P_{e^-}, P_{e^+}) = (0, 0)$ and b) polarized electron-positron beam $(P_{e^-}, P_{e^+}) = (-80\%, 60\%)$. In the first scenario, the unpolarized

TABLE IV: Sensitivity estimates on the μ_{ν_τ} magnetic moment and d_{ν_τ} electric dipole moment via the process $e^+e^- \rightarrow \nu_\tau \bar{\nu}_\tau \gamma$ for $\sqrt{s} = 380 \text{ GeV}$, $P_{e^-} = -80\%$ and $P_{e^-} = 60\%$.

90% C.L. $\sqrt{s} = 380 \text{ GeV}$						
$\delta_{sys} = 0\%$			$\delta_{sys} = 5\%$		$\delta_{sys} = 10\%$	
$\mathcal{L} (fb^{-1})$	$ \mu_{\nu_\tau}(\mu_B) $	$ d_{\nu_\tau}(ecm) $	$ \mu_{\nu_\tau}(\mu_B) $	$ d_{\nu_\tau}(ecm) $	$ \mu_{\nu_\tau}(\mu_B) $	$ d_{\nu_\tau}(ecm) $
10	7.563×10^{-6}	1.465×10^{-16}	9.467×10^{-6}	1.592×10^{-16}	1.059×10^{-5}	1.735×10^{-16}
50	5.684×10^{-6}	1.101×10^{-16}	8.485×10^{-6}	1.425×10^{-16}	1.043×10^{-5}	1.644×10^{-16}
100	4.980×10^{-6}	9.651×10^{-17}	8.414×10^{-6}	1.394×10^{-16}	1.041×10^{-5}	1.394×10^{-16}
300	3.993×10^{-6}	7.737×10^{-17}	8.365×10^{-6}	1.372×10^{-16}	1.039×10^{-5}	1.621×10^{-16}
500	3.585×10^{-6}	6.948×10^{-17}	8.355×10^{-6}	1.367×10^{-16}	1.038×10^{-5}	1.619×10^{-16}
95% C.L. $\sqrt{s} = 380 \text{ GeV}$						
$\delta_{sys} = 0\%$			$\delta_{sys} = 5\%$		$\delta_{sys} = 10\%$	
$\mathcal{L} (fb^{-1})$	$ \mu_{\nu_\tau}(\mu_B) $	$ d_{\nu_\tau}(ecm) $	$ \mu_{\nu_\tau}(\mu_B) $	$ d_{\nu_\tau}(ecm) $	$ \mu_{\nu_\tau}(\mu_B) $	$ d_{\nu_\tau}(ecm) $
10	8.018×10^{-6}	1.553×10^{-16}	9.467×10^{-6}	1.834×10^{-16}	1.117×10^{-5}	2.163×10^{-16}
50	6.061×10^{-6}	1.174×10^{-16}	8.975×10^{-6}	1.739×10^{-16}	1.099×10^{-5}	2.130×10^{-16}
100	5.326×10^{-6}	1.032×10^{-16}	8.902×10^{-6}	1.725×10^{-16}	1.097×10^{-5}	2.126×10^{-16}
300	4.289×10^{-6}	8.312×10^{-17}	8.851×10^{-6}	1.715×10^{-16}	1.096×10^{-5}	2.123×10^{-16}
500	3.860×10^{-6}	7.479×10^{-17}	8.841×10^{-6}	1.713×10^{-16}	1.095×10^{-5}	2.122×10^{-16}

cross section has the value of $\approx 200(200) \text{ pb}$ (see Figs. 2 and 3) depending on the anomalous coupling type F_2 (F_3). In the second scenario, which is motivated by the possibility to enhance or suppress different physical processes, the polarized cross section gets a value of $\approx 300(300) \text{ pb}$ (see Figs. 7 and 8) depending on the anomalous coupling type F_2 (F_3). Comparing each scenario shows that the cross section is enhanced for 100 pb for the case of polarized electron-positron beam. The option of upgrading the incoming electron and the positron beam to be polarized has the power to enhance the potential of the machine. In addition to these, the results for the sensitivity contours in the $F_2 - F_3$ plane for the unpolarized and polarized case are presented (see Figs. 4-6 and 9-11).

TABLE V: Sensitivity estimates on the μ_{ν_τ} magnetic moment and d_{ν_τ} electric dipole moment via the process $e^+e^- \rightarrow \nu_\tau \bar{\nu}_\tau \gamma$ for $\sqrt{s} = 1500 \text{ GeV}$, $P_{e^-} = -80\%$ and $P_{e^+} = 60\%$.

90% C.L. $\sqrt{s} = 1500 \text{ GeV}$						
$\delta_{sys} = 0\%$			$\delta_{sys} = 5\%$		$\delta_{sys} = 10\%$	
$\mathcal{L} (fb^{-1})$	$ \mu_{\nu_\tau}(\mu_B) $	$ d_{\nu_\tau}(ecm) $	$ \mu_{\nu_\tau}(\mu_B) $	$ d_{\nu_\tau}(ecm) $	$ \mu_{\nu_\tau}(\mu_B) $	$ d_{\nu_\tau}(ecm) $
10	1.503×10^{-6}	2.912×10^{-17}	1.654×10^{-6}	3.206×10^{-17}	1.926×10^{-6}	3.732×10^{-17}
100	8.940×10^{-7}	1.732×10^{-17}	1.379×10^{-6}	2.673×10^{-17}	1.805×10^{-6}	3.498×10^{-17}
500	6.085×10^{-7}	1.179×10^{-17}	1.341×10^{-6}	2.600×10^{-17}	1.792×10^{-6}	3.474×10^{-17}
1000	5.140×10^{-7}	9.960×10^{-18}	1.336×10^{-6}	2.590×10^{-17}	1.791×10^{-6}	3.471×10^{-17}
1500	4.654×10^{-7}	9.018×10^{-18}	1.335×10^{-6}	2.587×10^{-17}	1.790×10^{-6}	3.469×10^{-17}
95% C.L. $\sqrt{s} = 1500 \text{ GeV}$						
$\delta_{sys} = 0\%$			$\delta_{sys} = 5\%$		$\delta_{sys} = 10\%$	
$\mathcal{L} (fb^{-1})$	$ \mu_{\nu_\tau}(\mu_B) $	$ d_{\nu_\tau}(ecm) $	$ \mu_{\nu_\tau}(\mu_B) $	$ d_{\nu_\tau}(ecm) $	$ \mu_{\nu_\tau}(\mu_B) $	$ d_{\nu_\tau}(ecm) $
10	1.618×10^{-6}	3.137×10^{-17}	1.779×10^{-6}	3.447×10^{-17}	2.064×10^{-6}	4.000×10^{-17}
100	9.698×10^{-7}	1.879×10^{-17}	1.488×10^{-6}	2.883×10^{-17}	1.937×10^{-6}	3.754×10^{-17}
500	6.620×10^{-7}	1.282×10^{-17}	1.448×10^{-6}	2.886×10^{-17}	1.924×10^{-6}	3.728×10^{-17}
1000	5.596×10^{-7}	1.084×10^{-17}	1.442×10^{-6}	2.795×10^{-17}	1.923×10^{-6}	3.725×10^{-17}
1500	5.069×10^{-7}	9.823×10^{-18}	1.440×10^{-6}	2.792×10^{-17}	1.922×10^{-6}	3.724×10^{-17}

Figs. 2-11 and Tables I-VI highlight that sensitivity estimates for the total cross section, the form factors $F_2(F_3)$, as well as for the anomalous μ_{ν_τ} and d_{ν_τ} at CLIC for high center-of-mass energies and high luminosities, they reach a better sensitivity to that of L3 [69], CERN-WA-066 [70] and E872 (DONUT) [22], as well as of others experimental and theoretical results (see Table I of Ref. [26]). The most optimistic scenario about the sensitivity in the anomalous dipole moments of the τ -neutrino (see Tables III and VI), yields the following results: $|\mu_{\nu_\tau}(\mu_B)| = 2.103 \times 10^{-7}$ and $|d_{\nu_\tau}(ecm)| = 4.076 \times 10^{-18}$ with $(P_{e^-}, P_{e^+}) = (0\%, 0\%)$. In addition, we also obtain the results $|\mu_{\nu_\tau}(\mu_B)| = 2.002 \times 10^{-7}$ and $|d_{\nu_\tau}(ecm)| = 4.039 \times 10^{-18}$ with $(P_{e^-}, P_{e^+}) = (-80\%, 60\%)$. Our results show the potential and the feasibility of the

TABLE VI: Sensitivity estimates on the μ_{ν_τ} magnetic moment and d_{ν_τ} electric dipole moment via the process $e^+e^- \rightarrow \nu_\tau \bar{\nu}_\tau \gamma$ for $\sqrt{s} = 3000 \text{ GeV}$, $P_{e^-} = -80\%$ and $P_{e^+} = 60\%$.

90% C.L. $\sqrt{s} = 3000 \text{ GeV}$						
$\delta_{sys} = 0\%$			$\delta_{sys} = 5\%$		$\delta_{sys} = 10\%$	
$\mathcal{L} (fb^{-1})$	$ \mu_{\nu_\tau}(\mu_B) $	$ d_{\nu_\tau}(ecm) $	$ \mu_{\nu_\tau}(\mu_B) $	$ d_{\nu_\tau}(ecm) $	$ \mu_{\nu_\tau}(\mu_B) $	$ d_{\nu_\tau}(ecm) $
100	4.609×10^{-7}	9.276×10^{-18}	5.735×10^{-7}	1.160×10^{-17}	7.284×10^{-7}	1.475×10^{-17}
500	3.116×10^{-7}	6.281×10^{-18}	5.235×10^{-7}	1.064×10^{-17}	7.085×10^{-7}	1.437×10^{-17}
1000	2.628×10^{-7}	5.299×10^{-18}	5.161×10^{-7}	1.049×10^{-17}	7.059×10^{-7}	1.432×10^{-17}
2000	2.214×10^{-7}	4.465×10^{-18}	5.122×10^{-7}	1.042×10^{-17}	7.046×10^{-7}	1.429×10^{-17}
3000	2.002×10^{-7}	4.039×10^{-18}	5.109×10^{-7}	1.039×10^{-17}	7.041×10^{-7}	1.428×10^{-17}
95% C.L. $\sqrt{s} = 3000 \text{ GeV}$						
$\delta_{sys} = 0\%$			$\delta_{sys} = 5\%$		$\delta_{sys} = 10\%$	
$\mathcal{L} (fb^{-1})$	$ \mu_{\nu_\tau}(\mu_B) $	$ d_{\nu_\tau}(ecm) $	$ \mu_{\nu_\tau}(\mu_B) $	$ d_{\nu_\tau}(ecm) $	$ \mu_{\nu_\tau}(\mu_B) $	$ d_{\nu_\tau}(ecm) $
100	5.010×10^{-7}	1.007×10^{-17}	6.223×10^{-7}	1.258×10^{-17}	7.883×10^{-7}	1.595×10^{-17}
500	3.394×10^{-7}	6.840×10^{-18}	5.686×10^{-7}	1.154×10^{-17}	7.671×10^{-7}	1.554×10^{-17}
1000	2.863×10^{-7}	5.773×10^{-18}	5.605×10^{-7}	1.139×10^{-17}	7.642×10^{-7}	1.549×10^{-17}
2000	2.413×10^{-7}	4.867×10^{-18}	5.564×10^{-7}	1.131×10^{-17}	7.628×10^{-7}	1.546×10^{-17}
3000	2.183×10^{-7}	4.403×10^{-18}	5.549×10^{-7}	1.128×10^{-17}	7.623×10^{-7}	1.545×10^{-17}

process $e^+e^- \rightarrow \nu_\tau \bar{\nu}_\tau \gamma$ at the CLIC.

In conclusion, the process itself is very useful to sensitivity probing on the dipole moments of the tau-neutrino and illustrates the complementarity between CLIC and other e^+e^- and pp colliders for probing extensions of the SM. Furthermore, we hope that this work will motivate further studies of the $e^+e^- \rightarrow \nu_\tau \bar{\nu}_\tau \gamma$ process, using in particular polarized electron-positron beams.

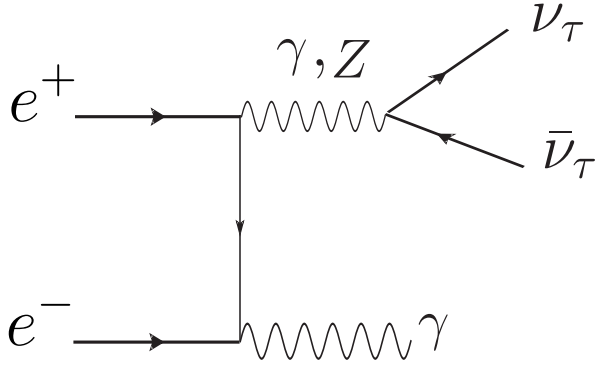
Acknowledgments

A. G. R. and M. A. H. R. acknowledges support from SNI and PROFOCIE (México).

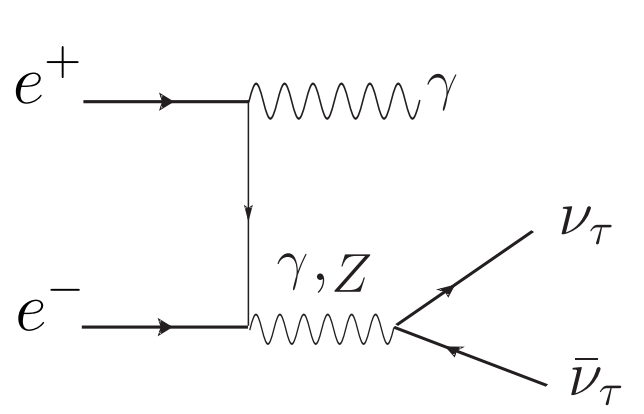
-
- [1] S. L. Glashow, *Nucl. Phys.* **22**, 579 (1961).
 - [2] S. Weinberg, *Phys. Rev. Lett.* **19**, 1264 (1967).
 - [3] A. Salam, in *Elementary Particle Theory*, Ed. N. Svartholm (Almquist and Wiskell, Stockholm, 1968) 367.
 - [4] K. Fujikawa and R. Shrock, *Phys. Rev. Lett.* **45**, 963 (1980).
 - [5] Robert E. Shrock, *Nucl. Phys.* **B206**, 359 (1982).
 - [6] J. H. Christenson, J. W. Cronin, V. L. Fitch, and R. Turlay, *Phys. Rev. Lett.* **13**, 138 (1964).
 - [7] K. Abe, *et al.*, *Phys. Rev. Lett.* **87**, 091802 (2001).
 - [8] R. Aaij, *et al.* [LHCb Collaboration], *J. High Energy Phys.* **07** (2014) 041.
 - [9] C. Patrignani, *et al.*, [Particle Data Group], *Chin. Phys.* **C40**, 100001 (2016).
 - [10] A. Cisneros, *Astrophys. Space Sci.* **10**, 87 (1971).
 - [11] G. G. Raffelt, *Phys Rep.* **320**, (1999) 319.
 - [12] N. Yamanaka, *Analysis of the Electric Dipole Moment in the R-parity Violating Supersymmetric Standard Model*, Springer, Berlin Germany (2014). doi:10.1007/978-4-431-54544-6.
 - [13] N. Yamanaka, B. Sahoo, N. Yoshinaga, T. Sato, K. Asahi, and B. Das, *Eur. Phys. J.* **A53**, 54 (2017).
 - [14] T. E. Chupp, P. Fierlinger, M. J. Ramsey-Musolf and J. T. Singh, arXiv:1710.02504 [physics.atom-ph].
 - [15] J. Engel, M. J. Ramsey-Musolf, and U. van Kolck, *Prog. Part. Nucl. Phys.* **71**, 21 (2013).
 - [16] A. D. Sakharov, *Pisma Zh. Eksp. Teor. Fiz.* **5**, 32 (1967); *JETP Lett.* **5**, 24 (1967); *Sov. Phys. Usp.* **34**, 392 (1991); *Usp. Fiz. Nauk* **161**, 61 (1991).
 - [17] M. Zralek, *Acta Phys. Polon.* **B28**, 2225 (1997) [hep-ph/9711506].
 - [18] Z. Daraktchieva, *et al.*, [MUNU Collaboration], *Phys. Lett.* **B615**, 153 (2005).
 - [19] H. T. Wong, H. B. Li, S. T. Lin, *et al.*, [TEXONO Collaboration], *Phys. Rev.* **D75**, 012001 (2007).
 - [20] A. G. Beda, V. B. Brudanin, V. G. Egorov, *et al.*, [GEMMA Collaboration], *Adv. High Energy Phys.* **2012**, 350150 (2012).
 - [21] L. B. Auerbach, *et al.*, [LSND Collaboration], *Phys Rev.* **D63**, (2001) 112001, hep-ex/0101039.
 - [22] R. Schwinnhorst, *et al.*, [DONUT Collaboration], *Phys. Lett.* **B513**, 23 (2001).

- [23] C. Arpesella, *et al.*, [Borexino Collaboration], *Phys. Rev. Lett.* **101**, 091302 (2008).
- [24] D. W. Liu, *et al.*, [Super-Kamiokande Collaboration], *Phys. Rev. Lett.* **2**, 021802 (2004).
- [25] F. del Aguila and M. Sher, *Phys Lett.* **B252**, (1990) 116.
- [26] A. Gutiérrez-Rodríguez, M. Koksál, A. A. Billur, and M. A. Hernández-Ruíz, arXiv:1712.02439 [hep-ph].
- [27] A. A. Billur, M. Köksal, A. Gutiérrez-Rodríguez and M. A. Hernández-Ruíz, arXiv:1807.00238 [hep-ph].
- [28] A. Llamas-Bugarin, *et al.*, *Phys. Rev.* **D95**, 116008 (2017).
- [29] A. Gutiérrez-Rodríguez, M. Koksál and A. A. Billur, *Phys. Rev.* **D91**, 093008 (2015).
- [30] A. Gutiérrez-Rodríguez, M. Koksál and A. A. Billur, *PoS EPS-HEP2015*, 036 (2015), C15-07-22 Proceedings.
- [31] A. Gutiérrez-Rodríguez, *Int. J. Theor. Phys.* **54**, (2015) 236.
- [32] A. Gutiérrez-Rodríguez, *Advances in High Energy Physics* **2014**, 491252 (2014).
- [33] A. Gutiérrez-Rodríguez, *Pramana Journal of Physics* **79**, 903 (2012).
- [34] A. Gutiérrez-Rodríguez, *Eur. Phys. J.* **C71**, 1819 (2011).
- [35] C. Aydin, M. Bayar and N. Kilic, *Chin. Phys.* **C32**, 608 (2008).
- [36] A. Gutiérrez-Rodríguez, *et al.*, *Phys. Rev.* **D74**, 053002 (2006).
- [37] A. Gutiérrez-Rodríguez, *et al.*, *Phys. Rev.* **D69**, 073008 (2004).
- [38] A. Gutiérrez-Rodríguez, *et al.*, *Acta Physica Slovaca* **53**, 293 (2003).
- [39] K. Akama, T. Hattori and K. Katsuura, *Phys. Rev. Lett.* **88**, 201601 (2002).
- [40] A. Aydemir and R. Sever, *Mod. Phys. Lett.* **A16** 7, 457 (2001).
- [41] A. Gutiérrez-Rodríguez, *et al.*, *Rev. Mex. de Fís.* **45**, 249 (1999).
- [42] A. Gutiérrez-Rodríguez, *et al.*, *Phys. Rev.* **D58**, 117302 (1998).
- [43] P. Abreu, *et al.*, [DELPHI Collaboration], *Z. Phys.* **C74**, 577 (1997).
- [44] R. Escribano and E. Massó, *Phys. Lett.* **B395**, 369 (1997).
- [45] T. M. Gould and I. Z. Rothstein, *Phys. Lett.* **B333**, 545 (1994).
- [46] H. Grotch and R. Robinet, *Z. Phys.* **C39**, 553 (1988).
- [47] I. Sahin, *Phys. Rev.* **D85**, 033002 (2012).
- [48] I. Sahin and M. Koksál, *JHEP* **03**, 100 (2011).
- [49] E. Accomando, *et al.* (CLIC Phys. Working Group Collaboration), arXiv: hep-ph/0412251, CERN-2004-005.

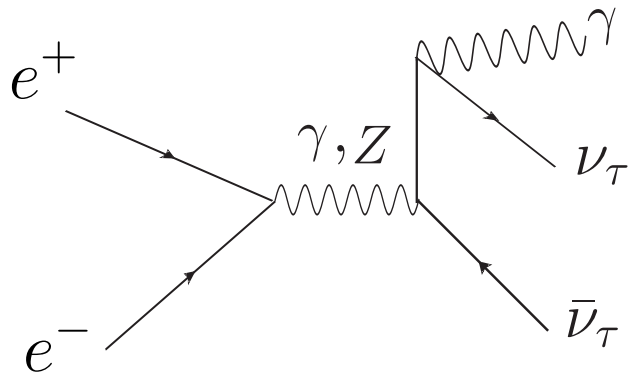
- [50] D. Dannheim, P. Lebrun, L. Linssen, *et al.*, arXiv: 1208.1402 [hep-ex].
- [51] H. Abramowicz, *et al.*, (CLIC Detector and Physics Study Collaboration), arXiv:1307.5288 [hep-ex].
- [52] J. F. Nieves, *Phys. Rev.* **D26**, 3152 (1982).
- [53] B. Kayser, A. Goldhaber, *Phys. Rev.* **D28**, 2341 (1983).
- [54] B. Kayser, *Phys. Rev.* **D30**, 1023 (1984).
- [55] C. Giunti and A. Studenikin, *Rev. Mod. Phys.* **87**, 531(2015).
- [56] P. Vogel and J. Engel, *Phys. Rev.* **D39**, 3378 (1989).
- [57] J. Bernabeu, *et al.*, *Phys. Rev.* **D62**, 113012 (2000).
- [58] J. Bernabeu, *et al.*, *Phys. Rev. Lett.* **89**, 101802 (2000).
- [59] M. S. Dvornikov and A. I. Studenikin, *Jour. of Exp. and Theor. Phys.* **99**, 254 (2004).
- [60] C. Brogini, C. Giunti, A. Studenikin, *Adv. High Energy Phys.* **2012**, (2012) 459526.
- [61] A. Belyaev, N. D. Christensen and A. Pukhov, *Comput. Phys. Commun.* **184**, 1729 (2013).
- [62] M. Köksal, A. A. Billur, A. Gutiérrez-Rodríguez and M. A. Hernández-Ruíz, *Phys. Rev.* **D98**, 015017 (2018).
- [63] M. Köksal, S. C. Inan, A. A. Billur, Y. Özgüven and M. K. Bahar, *Phys. Lett.* **B783**, 375 (2018).
- [64] M. Köksal, A. A. Billur and A. Gutiérrez-Rodríguez, *Adv. High Energy Phys.* **2017**, 6738409 (2017).
- [65] Y. Özgüven, S. C. Inan, A. A. Billur, M. Köksal, M. K. Bahar, *Nucl. Phys.* **B923**, 475 (2017).
- [66] A. A. Billur, M. Köksal and A. Gutiérrez-Rodríguez, *Phys. Rev.* **D96**, 056007 (2017).
- [67] A. A. Billur, M. Köksal, *Phys. Rev.* **D89**, 037301 (2014).
- [68] G. Moortgat-Pick, *et al.*, *Phys. Rept.* **460**, 131 (2008).
- [69] M. Acciarri *et al.*, [L3 Collaboration], *Phys. Lett.* **B412**, 201 (1997).
- [70] A. M. Cooper-Sarkar, *et al.*, [WA66 Collaboration], *Phys. Lett.* **B280**, 153 (1992).



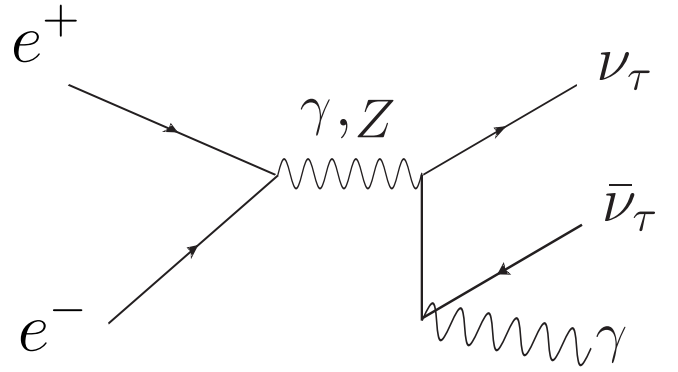
(1, 2)



(3, 4)



(5, 6)



(7, 8)

FIG. 1: The Feynman diagrams for the process $e^+e^- \rightarrow (\gamma, Z) \rightarrow \nu_\tau \bar{\nu}_\tau \gamma$.

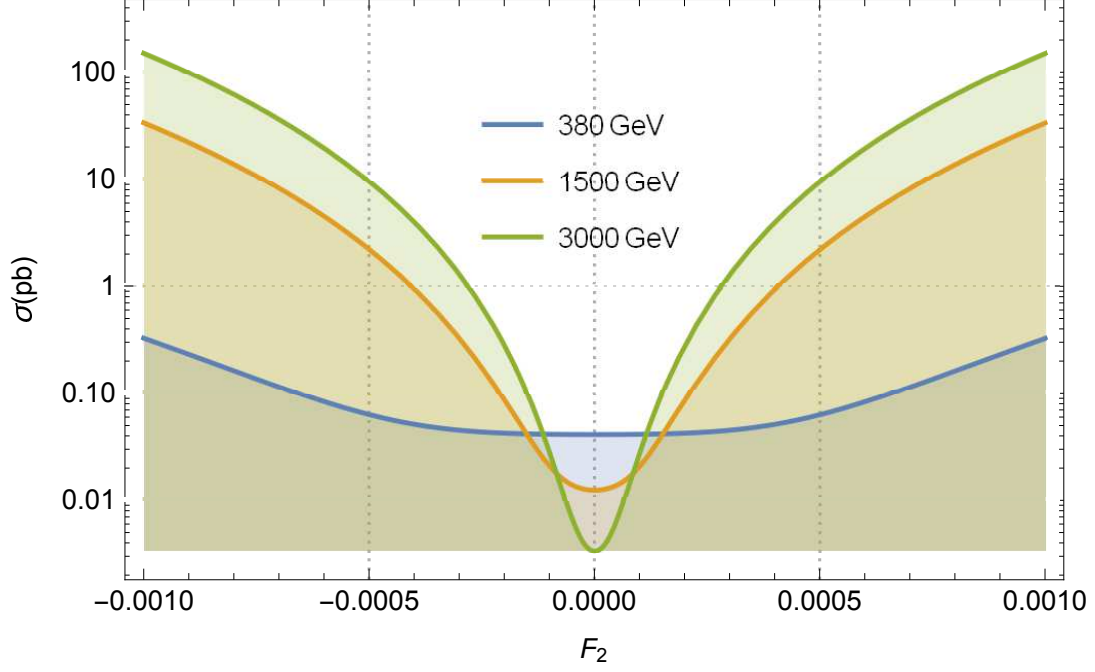


FIG. 2: The total cross sections of the process $e^+e^- \rightarrow \nu_\tau \bar{\nu}_\tau \gamma$ as a function of F_2 for center-of-mass energies of $\sqrt{s} = 380, 1500, 3000 \text{ GeV}$.

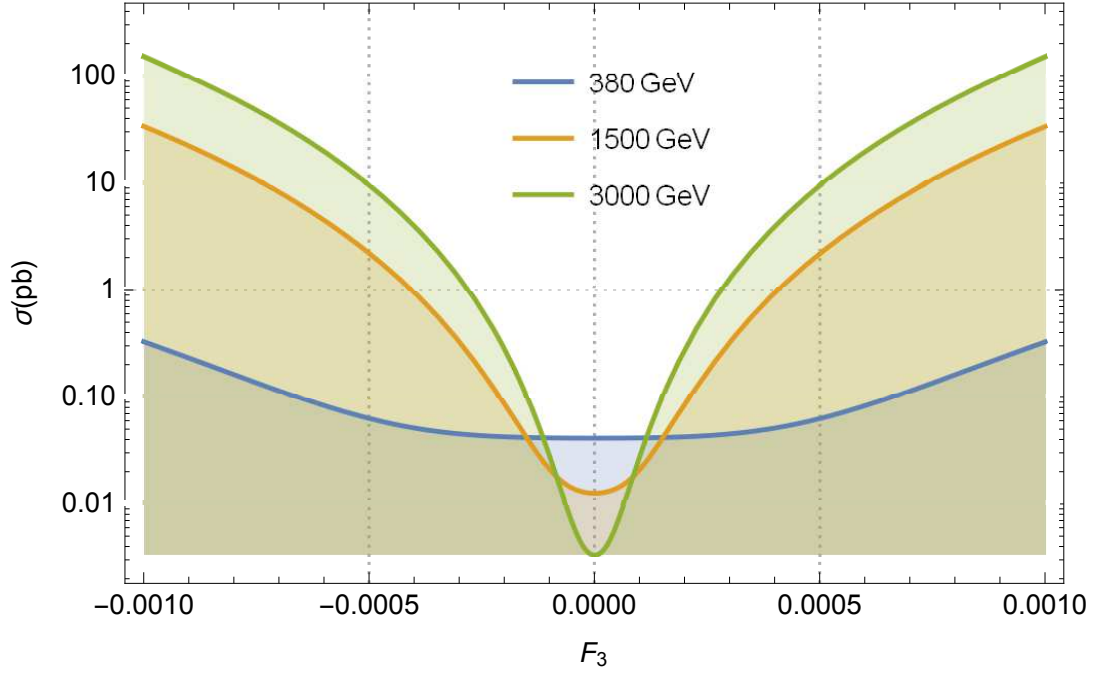


FIG. 3: Same as in Fig. 2, but for F_3 .

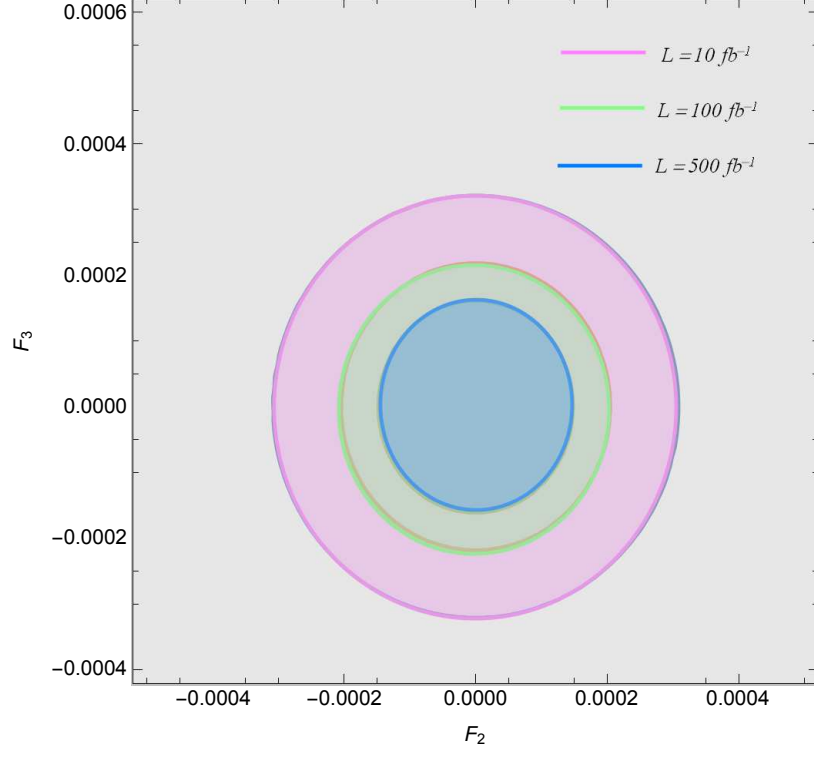


FIG. 4: Sensitivity contours at the 95% *C.L.* in the $F_3 - F_2$ plane for the process $e^+e^- \rightarrow \nu_\tau \bar{\nu}_\tau \gamma$ with the $\delta_{sys} = 0\%$ and for center-of-mass energy of $\sqrt{s} = 380$ GeV.

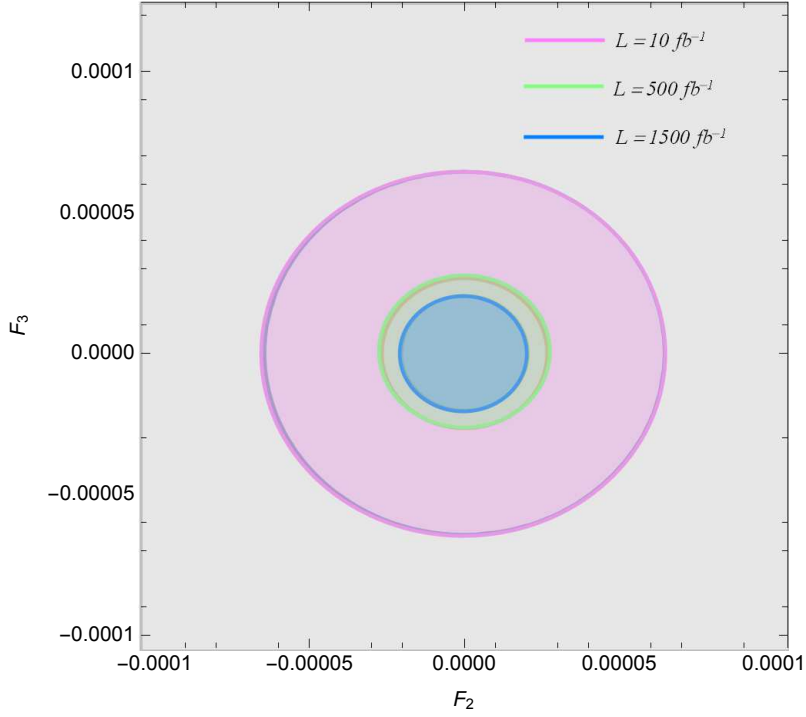


FIG. 5: Same as in Fig. 4, but for $\sqrt{s} = 1500$ GeV.

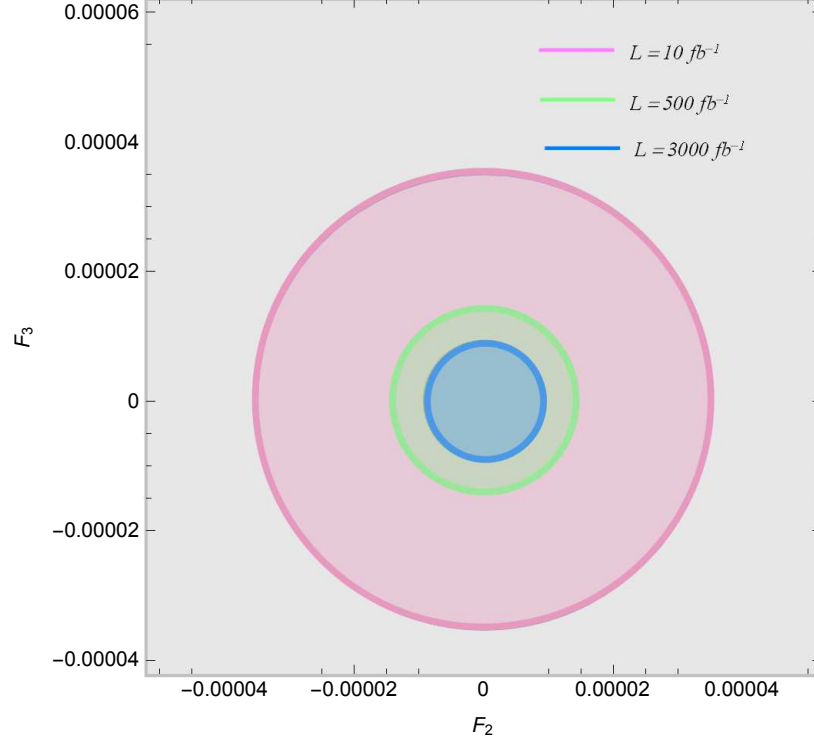


FIG. 6: Same as in Fig. 4, but for $\sqrt{s} = 3000 \text{ GeV}$.

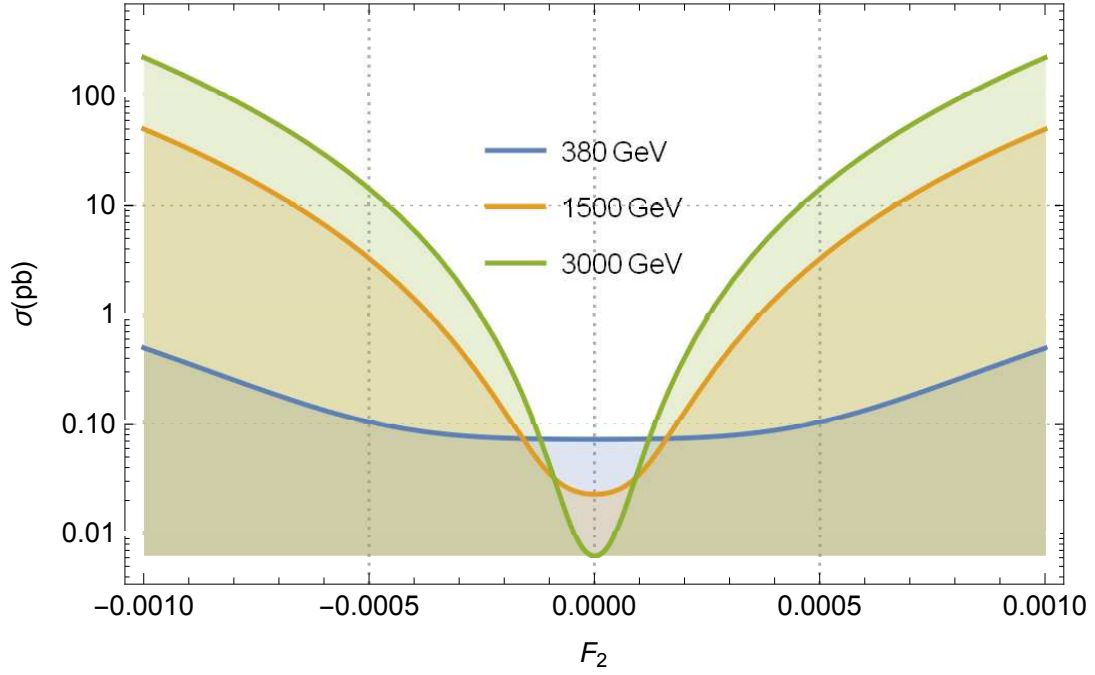


FIG. 7: Same as in Fig. 2, but for $P_{e^-} = -80\%$ and $P_{e^+} = 60\%$.

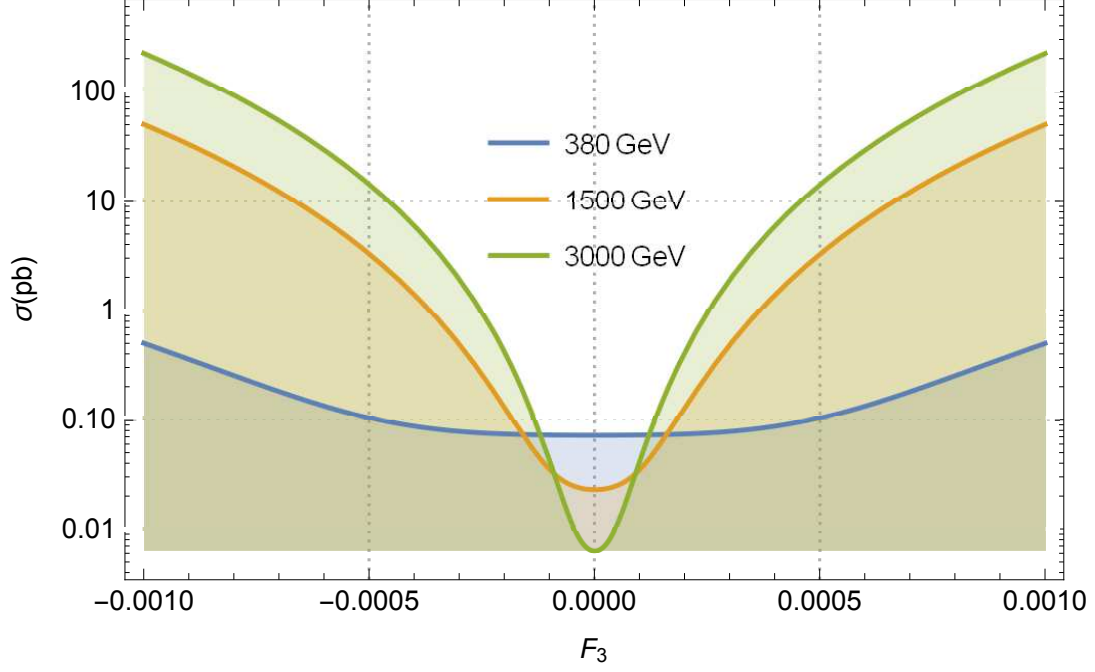


FIG. 8: Same as in Fig. 3, but for $P_{e^-} = -80\%$ and $P_{e^+} = 60\%$.

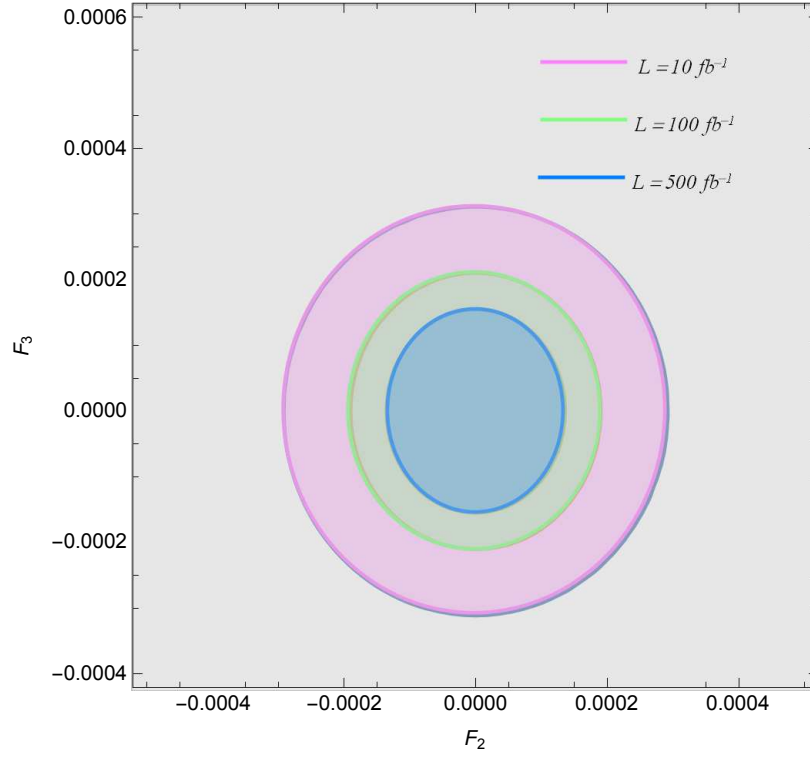


FIG. 9: Same as in Fig. 4, but for $P_{e^-} = -80\%$ and $P_{e^+} = 60\%$.

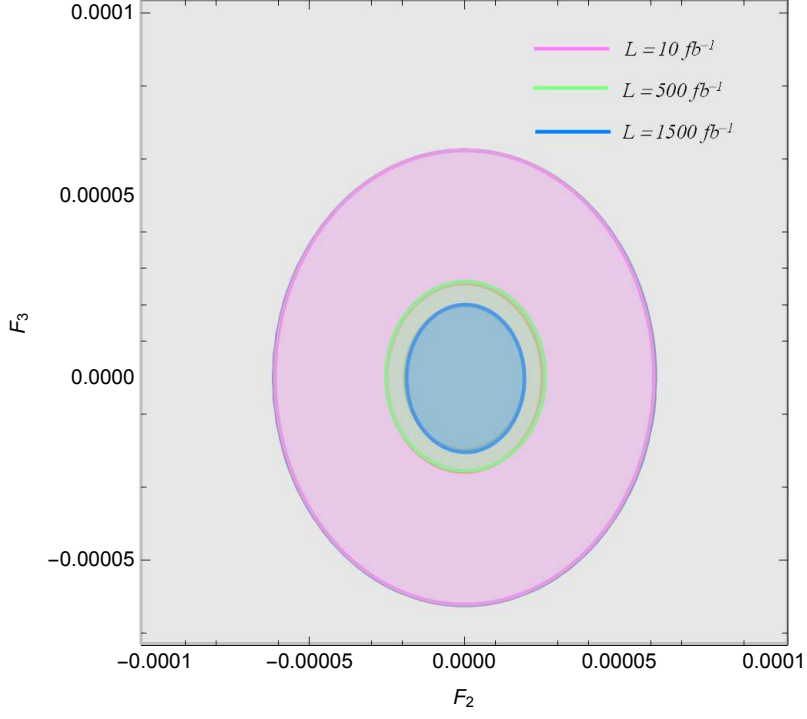


FIG. 10: Same as in Fig. 5, but for $P_{e-} = -80\%$ and $P_{e+} = 60\%$.

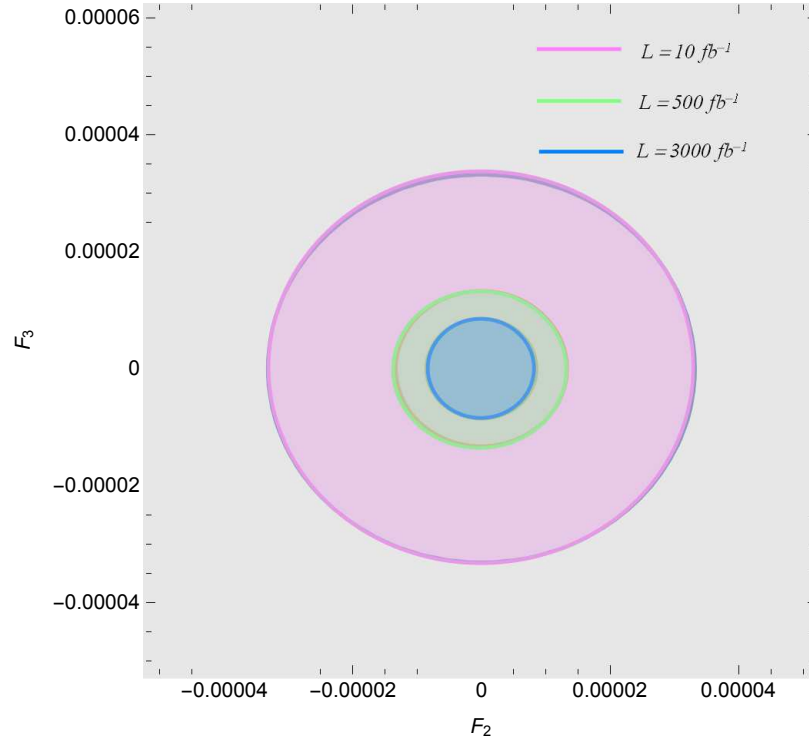


FIG. 11: Same as in Fig. 6, but for $P_{e-} = -80\%$ and $P_{e+} = 60\%$.